PHYSICAL REVIEW D **96,** 015010 (2017)

QCD-improved limits from neutrinoless double beta decay

C. Arbeláez,[*] M. González,[†] and S. G. Kovalenko[‡]
Universidad Técnica Federico Santa María, Centro-Científico-Tecnológico de Valparaíso, Casilla 110-V, Valparaíso, Chile

M. Hirsch[§]
AHEP Group, Instituto de Física Corpuscular—C.S.I.C./Universitat de València Edificio de Institutos de Paterna, Apartado 22085, E–46071 València, Spain
(Received 24 November 2016; published 11 July 2017)

We analyze the impact of QCD corrections on limits derived from neutrinoless double beta decay ($0\nu\beta\beta$). As demonstrated previously, the effect of the color mismatch arising from loops with gluons linking the quarks from different color-singlet currents participating in the effective operators has a dramatic impact on the predictions for some particular Wilson coefficients. Here, we consider all possible contributions from heavy particle exchange, i.e. the so-called short-range mechanism of $0\nu\beta\beta$ decay. All high-scale models (HSM) in this class match at some scale around a $\sim$ few TeV with the corresponding effective theory, containing a certain set of effective dimension-9 operators. Many of these HSM receive contributions from more than one of the basic operators and we calculate limits on these models using the latest experimental data. We also show with one nontrivial example, how to derive limits on more complicated models, in which many different Feynman diagrams contribute to $0\nu\beta\beta$ decay, using our general method.

DOI: 10.1103/PhysRevD.96.015010

I. INTRODUCTION

Lepton number violation (LNV) appears in many extensions of the Standard Model (SM). If LNV exists, it could be the explanation for the smallness of the observed neutrino masses and maybe even the baryon asymmetry of the universe [1]. Neutrinoless double beta decay ($0\nu\beta\beta$) is widely credited as the most promising probe for LNV from the view point of experimental observability. Consequently, $0\nu\beta\beta$-decay has been studied in great detail, both from theoretical and experimental points of view.[1]

A number of experiments are currently searching for $0\nu\beta\beta$-decay [6–10] with the negative results setting lower bounds on the $0\nu\beta\beta$-half-life $T^{0\nu}_{1/2}$. Currently the best bounds are

$$\text{KamLAND-Zen [9]: } T^{0\nu}_{1/2}(^{136}\text{Xe}) = 1.07 \times 10^{26}\ \text{ys(90\% C.L.)}, \quad (1)$$

$$\text{GERDA Phase-II [10]: } T^{0\nu}_{1/2}(^{76}\text{Ge}) = 5.2 \times 10^{25}\ \text{ys(90\%C.L.)}. \quad (2)$$

Sensitivities in excess of $T^{0\nu}_{1/2} \gtrsim 10^{27}$ ys in experiments using ^{136}Xe [11] and ^{76}Ge [12,13] are expected in the future.

Contributions to $0\nu\beta\beta$-decay can be classified as either long-range (LRM) [14] or short-range mechanisms (SRM) [15], depending on whether all of the virtually exchanged particles are heavy or not, see Fig. 1. For the short-range mechanisms, SRM, the experimental limits imply typical masses of heavy intermediate particles and an LNV scale Λ_{LNV} in the ballpark of (a few) TeV. Therefore, the LHC could possibly provide a cross-check whether or not these contributions can be dominant in $0\nu\beta\beta$-decay [16–20].

Naturally, for a realistic comparison of the sensitivities of the $0\nu\beta\beta$-decay experiments with the LHC ones the theoretical calculations must be made as reliable as possible, which is particularly demanding for $0\nu\beta\beta$-decay. One well-known source of difficulties in this case are uncertainties in the Nuclear Matrix Elements (NME),

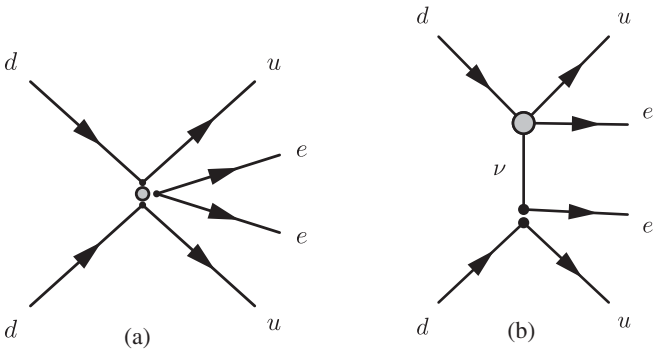

FIG. 1. Short-range mechanism (SRM), to the left, and long-range mechanism (LRM) to the right. The grey blobs indicate effective vertices originating from heavy particle-exchange.

[*]carolina.arbelaez@usm.cl
[†]marcela.gonzalezp@usm.cl
[‡]sergey.kovalenko@usm.cl
[§]mahirsch@ific.uv.es

[1]For reviews of particle physics aspects of $0\nu\beta\beta$ see for instance Refs. [2,3] and for recent calculations of nuclear matrix elements Refs. [4,5].

which spread by a factor of typically ∼2 comparing different calculations. Improving the predictions for $0\nu\beta\beta$-NMEs is a serious challenge for nuclear structure theory, which is going to take time and significant efforts. On the other hand, recently it has been pointed out that one important effect has so far been missing in the theoretical treatment of $0\nu\beta\beta$-decay [21,22]: QCD corrections. This effect, being perturbative, is much better controllable theoretically than the essentially nonperturbative (in quantum field theory sense) physics involved in the NME calculations. As explained in Ref. [22] gluon exchange diagrams can lead to the so called "color-mismatch" in the products of the color-singlet quark currents giving rise to an appreciable mixing between different $0\nu\beta\beta$-effective operators. The vastly differing numerical values of NMEs for different operators then result in dramatic changes of the limits on the Wilson coefficients of some particular operators. This feature is pertinent to the SRMs of $0\nu\beta\beta$-decay. It has been recently demonstrated in Ref. [23] that the color-mismatch effect is absent in the case of the LRMs of $0\nu\beta\beta$-decay and, therefore, for this class of mechanisms the QCD corrections are not so crucial.

For such a fairly low-energy process as $0\nu\beta\beta$-decay an effective operator description is adequate for calculating the decay rate. This rather straightforward observation forms the framework of the original papers [14,15] where the basis of the effective $0\nu\beta\beta$-decay $d=9$ operators was introduced and generic formulas for the $0\nu\beta\beta$-decay half-life were derived. More recently this approach has been developed in Refs. [22,23] where we derived the QCD-corrected $0\nu\beta\beta$-decay half-life formulas for both SRM and LRM.[2] From the more fundamental high-energy point of view, however, contributions to $0\nu\beta\beta$-decay originate from some renormalizable LNV extension of the SM, i.e. high-scale models (HSM), whose parameters are the couplings and masses of experimentally yet unknown particles.

A list of all possible HSMs representing UV completions of the above-mentioned $0\nu\beta\beta$-decay $d=9$ operators was given in Ref. [26] and from that paper, in principle, all the HSMs contributing to $0\nu\beta\beta$-decay via the short-range mechanism can be found. The purpose of our present paper is to provide a bridge between these two descriptions—in terms of the effective operators and the HSMs—taking into account the effect of the above-mentioned QCD corrections. Upper limits derived on the Wilson coefficients of the $0\nu\beta\beta$-decay effective operators (low energy approach) [22] can be converted into lower limits on the mass scales of the HSMs listed in Ref. [26] and we provide tables of these limits, using updated experimental lower bounds on the $0\nu\beta\beta$-decay half-life, for all "elementary" HSMs (see Sec. III).

[2]In Ref. [24] the QCD corrections were taken into account to the pion-exchange mechanism [25] of $0\nu\beta\beta$-decay. However, the tensor operator contribution, suppressed in this mechanism, were erroneously treated in [24] to be proportional to the scalar one after incorrectly neglecting the Fiertz generated octet operators.

While these "translation rules" can be applied in a rather straightforward manner to any particular HSM, for which only one Feynman diagram contributes significantly, there are many example models in the literature where this is not the case. In the presence of more than one significant diagram a careful examination of their contributions to different operators is required for arriving at the correct answer. We will discuss one particular example—R-parity violating supersymmetry—in some detail, to demonstrate the usefulness of our approach.

This paper is organized as follows. In Sec. II we start by recalling the definitions for the QCD corrected half-life formula for $0\nu\beta\beta$-decay. This section summarizes the results of Ref. [22]. We then derive limits on "elementary" HSMs contributing to the short-range $0\nu\beta\beta$-decay mechanism in Sec. III. In Sec. IV we discuss how to derive limits in our approach on more complicated HSMs. As already mentioned, we choose the well-known example of R-parity violating SUSY. We conclude with a discussion of our results in Sec. V. Some more technical aspects of the calculation are delegated to an Appendix.

II. QCD RUNNING OF SHORT-RANGE MECHANISMS

The contribution of a HSM to $0\nu\beta\beta$-decay via heavy particle exchange we call the short-range mechanism (SRM), already mentioned in the Introduction. After integrating out the heavy degrees of freedom of a mass $\sim M_I$ at an energy-scale $\mu < M_I$, all the HSMs of the SRM category can be represented by the effective Lagrangian [15,22]

$$\mathcal{L}_{\text{eff}}^{0\nu\beta\beta} = \frac{G_F^2}{2m_p}\sum_{i,XY} C_i^{XY}(\mu)\cdot\mathcal{O}_i^{XY}(\mu), \tag{3}$$

with the complete set of dimension-9 $0\nu\beta\beta$-operators

$$\mathcal{O}_1^{XY} = 4(\bar{u}P_X d)(\bar{u}P_Y d)j, \tag{4}$$

$$\mathcal{O}_2^{XX} = 4(\bar{u}\sigma^{\mu\nu}P_X d)(\bar{u}\sigma_{\mu\nu}P_X d)j, \tag{5}$$

$$\mathcal{O}_3^{XY} = 4(\bar{u}\gamma^{\mu}P_X d)(\bar{u}\gamma_{\mu}P_Y d)j, \tag{6}$$

$$\mathcal{O}_4^{XY} = 4(\bar{u}\gamma^{\mu}P_X d)(\bar{u}\sigma_{\mu\nu}P_Y d)j^{\nu}, \tag{7}$$

$$\mathcal{O}_5^{XY} = 4(\bar{u}\gamma^{\mu}P_X d)(\bar{u}P_Y d)j_{\mu}, \tag{8}$$

where X, $Y = L$, R and the leptonic currents are

$$j = \bar{e}(1\pm\gamma_5)e^c, \qquad j_{\mu} = \bar{e}\gamma_{\mu}\gamma_5 e^c. \tag{9}$$

The Wilson coefficients C_i^{XY} can be expressed in terms of the parameters of a particular HSM at a scale $\Lambda\sim M_I$, called "matching scale." Note that some of $C_i(\Lambda)$ may

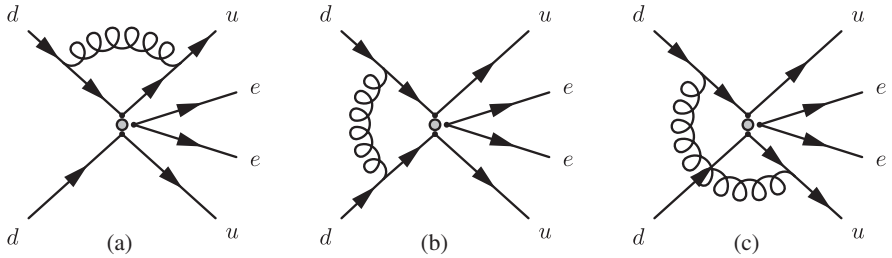

FIG. 2. One-loop QCD corrections to the short range mechanisms of $0\nu\beta\beta$ decay in the effective theory: the vertex renormalization (a) and the "color-mismatch" (b), (c) diagrams.

vanish. In order to make contact with $0\nu\beta\beta$-decay one needs to estimate C_i at a scale μ_0 close to the typical $0\nu\beta\beta$-energy scale. The QCD corrections, such as shown in Fig. 2, lead to running of the coefficients between the matching Λ and μ_0 scales.

While the QCD-running is only logarithmic, it mixes different operators (or equivalently Wilson coefficients) from the list (4)–(8). Because of the vast difference of the NMEs of some operators, this effect results in a dramatic impact on the prediction of some HSM for $0\nu\beta\beta$-decay [22].

On the way from the quark-level effective Lagrangian (3) to the NMEs one faces the problem of hadronization, namely, embedding the quark fields into effective hadronic ones. The underlying 4 quark operators $(\bar{u}d)(\bar{u}d)$ in Eqs. (4)–(8) can be hadronizated in various ways: into two nucleons or in one nucleon+one pion, or into two pions and so on. All these terms must be present in the effective low-energy hadronic Lagrangian. It is one of the big problems in $0\nu\beta\beta$-decay theory that we do not know the corresponding effective couplings, which depend on the as yet unknown hadronic wave functions. In such a situation it is a common lore, which we also adopt in our approach, to study the terms of the complete hadronic Lagrangian separately, as if there were only one way of hadronization and other terms were absent. We study the hadronization into two nucleons. References [25,27][3] focus on the nucleon-pion and pion-pion terms. However one should realize that they are complementary and separately do not reproduce the whole picture. As is known, in the nuclear media the pion terms/mechanism gain certain enhancement factors related, in particular, with its long-range nature and the presence of the nuclear short-range correlation. But it is currently unknown if the hadronization into pions is suppressed in comparison with nucleons or not. If yes, the pion mechanism might give less stringent constraints than what has been claimed in the literature so far. If not, one has to note that the pion-nucleon and pion-pion mechanisms are practically blind to the tensor operators appearing in many high-scale models. On the other hand the nucleon-nucleon mechanism is sensitive to all the Lorentz structures. Importantly, the NME of the tensor operators are about two orders of magnitude larger than, for example, the (pseudo-)scalar ones.

In summary of this discussion, in our analysis we deliberately neglect the pion mode of hadronization assuming it to be, for some reasons, suppressed in comparison with the nucleon mode. We are aware that this might not be the case, but this is also true for the studies based on the pion mode. We believe it is still an open—and crucial—question for $0\nu\beta\beta$-theory of how to correctly treat the hadronization of quark operators.

The $0\nu\beta\beta$-decay half-life formula, taking into account the leading order QCD-running [22], reads

$$[T^{0\nu\beta\beta}_{1/2}]^{-1} = G_1 \left| \sum_{i=1}^{3} \beta_i^{XY}(\mu_0,\Lambda) C_i^{XY}(\Lambda) \right|^2 + G_2 \left| \sum_{i=4}^{5} \beta_i^{XY}(\mu_0,\Lambda) C_i^{XY}(\Lambda) \right|^2 \quad (10)$$

Here, $G_{1,2}$ are phase space factors [15,28]. The summation over the different chiralities X, $Y = L$, R is implied. The parameters β_i^{XY} incorporate the QCD-running and the NMEs of the operators in Eqs. (4)–(8). Their explicit form is given in Appendix A. We show the values of these coefficients in Table I calculated with the NMEs from Ref. [2].[4] However, they can be easily recalculated for any other set of NMEs with Eqs. (A1)–(A11).

It is important to note that the Wilson coefficients $C_i(\Lambda)$, entering in Eq. (10), are linked to the matching scale Λ, where they are calculable in terms of the HSM parameters, such as couplings and intermediate particle masses.

In Ref. [22] we used the $0\nu\beta\beta$-decay half-life formula (10) in order to extract "individual" upper limits on the Wilson coefficients C_i^{XY} from the existing experimental bounds on $T^{0\nu\beta\beta}_{1/2}$. We employed the conventional hypothesis that a single term dominates in Eq. (10). This method disregards effects of a possible simultaneous presence of several nonzero terms, which may partially

[3]Ref. [27] ignores tensor × tensor or/and color $(\mathbf{8}\times\mathbf{8})_\mathbf{1}$ operators, crucial for some high-scale models.

[4]To our best knowledge there is no complete set of the NMEs published in the literature for all the operators (4)–(8) except for Ref. [2], which used the model of Ref. [29].

TABLE I. The coefficients $\beta_i \equiv \beta_i(\mu_0, \Lambda)$ incorporating NMEs and entering the QCD corrected half-life formula (10). The results are shown for the QCD running between the scales $\Lambda = 1$ TeV and $\mu_0 = 1$ GeV. See Appendix A.

Coefficients	Isotope ^{76}Ge	Isotope ^{136}Xe	Coefficients	Isotope ^{76}Ge	Isotope ^{136}Xe
β_1^{XX}	6.1×10^3	3.1×10^3	β_4^{XX}	$(-5.6 + 0.2i) \times 10^2$	$(-2.9 + 0.1i) \times 10^2$
β_1^{LR}	-2.5×10^2	-1.3×10^2	β_4^{LR}	1.2×10^2	6.0×10^1
β_2^{XX}	-4.4×10^2	-2.3×10^2	β_5^{XX}	$(0.9 - 1.3i) \times 10^2$	$(4.5 - 6.6i) \times 10^1$
β_3^{XX}	1.5×10^2	7.5×10^1	β_5^{LR}	7.7×10^1	3.9×10^1
β_3^{LR}	1.1×10^2	5.7×10^1			

cancel each other or give rise to a significant enhancement. These effects are discussed in the next section.

III. LIMITS ON SHORT-RANGE ELEMENTARY HIGH-SCALE MODELS

Two tree-level topologies contributing to the $0\nu\beta\beta$ decay amplitude were identified in Ref. [26], see Fig. 3. Here, the outer lines of the diagrams represent all possible permutations of the six fermions $\bar{u}\,\bar{u}\,dd\bar{e}\,\bar{e}$, which make up the $0\nu\beta\beta$ decay operator. Considering $G_{\rm SM} = SU(3)_c \times SU(2)_L \times U(1)_Y$ invariant vertices in these diagrams one may derive a complete list of the $G_{\rm SM}$-assignments for the intermediate particles $(\text{Scalar}, \text{Fermion}, \text{Scalar}) = (S, \Psi, S')$ and $(\text{three Scalars}) = (S, S', S'')$ in the T-I and T-II topology diagrams, respectively. This was done in Ref. [26]. Each case in this list we call "elementary" HSM (eHSM). We reproduce the original list of Ref. [26] in Tables VI, VII and IX where, for convenience of our analysis, we collected the eHSMs in groups enumerated by #I. Any short-range HSM can be represented in the form of a linear combination of several eHSMs. The HSMs considered in the literature (for a recent review cf. Ref. [2]) are mainly of this kind with the parameters (couplings, masses) of the involved eHSMs related between each other by symmetry or other arguments. We will discuss one example of such nonelementary HSM—$\not{R}_p$ SUSY—in the next section and here first focus on the eHSMs.

In the case of the short-range mechanism all the HSMs in the low-energy limit are reducible to the effective Lagrangian (3). By definition each eHSM generates, after integrating out heavy particles, a single effective operator. It is straightforward, although tedious, to check that all the eHSMs from each group #I in Tables VI, VII and IX lead to the same effective operator $\mathcal{O}^I$. Projection of $\mathcal{O}^I$ on the general operator basis $\mathcal{O}_i$ in Eqs. (4)–(8) via Lorentz and color Fierz transformations (see Appendix B) gives rise to a linear combination of only two basis operators

$$\mathcal{O}^I = x_i^I \mathcal{O}_i + y_j^I \mathcal{O}_j \tag{11}$$

with numerical coefficients x^I, y^I algebraically calculable for any particular eHSM [26]. Note that no summation over the repeated indices i, j is implied in Eq. (11). All of the possible operator pairs with the corresponding coefficients are shown in Tables II and III. Some eHSM lead to only one of the basis operators, these are listed in Table IV. The values of the coefficients x^I, y^I given in these Tables are useful as an additional identifier of the eHSMs as well as for recalculation of the experimental limits on the parameters of the eHSMs, also given in these Tables, with the NMEs and the experimental $0\nu\beta\beta$-decay half-life bounds different from those we used here.

We derived these limits in the following way. The effective Lagrangian for any #I eHSM at the matching scale Λ can be expressed, taking into account (11), as

$$\begin{aligned}\mathcal{L}_I &= \frac{G_F^2}{2m_p} C_I(\Lambda) \cdot \mathcal{O}^I(\Lambda) \\ &= \frac{G_F^2}{2m_p} C_I(\Lambda) \cdot (x_i^I \mathcal{O}_i(\Lambda) + y_j^I \mathcal{O}_j(\Lambda)).\end{aligned} \tag{12}$$

The half-life formula (10), used to constrain a concrete eHSM, is reduced to

$$T_{1/2}^{-1} = G_{K_I} |C_I(\Lambda)|^2 |\beta_i(\mu_0, \Lambda) x_i^I + \beta_j(\mu_0, \Lambda) y_j^I|^2. \tag{13}$$

Here $K_I = 1$ or 2 for $i, j \in \{1, 2, 3\}$ or for $i, j \in \{4, 5\}$, respectively.

Using the current experimental $0\nu\beta\beta$-decay half-life lower bounds (1), (2) we derive from Eq. (13) upper limits on the Wilson coefficients $C_I(\Lambda = 1\ \text{TeV}) \leq C_I^{\rm exp}$. These

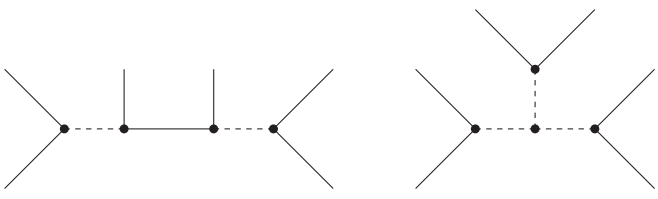

FIG. 3. Tree-level topologies contributing to the short-range mechanism of $0\nu\beta\beta$-decay. To the left T-I, boson-fermion-boson exchange; to the right T-II, triple-boson diagrams. External lines stand symbolically for any permutation of $\bar{u}\,\bar{u}\,dd\bar{e}\,\bar{e}$.

TABLE II. Decomposition in the basis operators (4)–(8) of the effective operators $\mathcal{O}^I$ representing low-energy limits of the eHSMs of the group # I specified in Tables VI–IX. Experimental limits on the Wilson Coefficients $C_I(\Lambda = 1\ \text{TeV}) \leq C_I^{\text{exp}}$ of these operators and their characteristic scales $M_I \geq \lambda_{\text{eff}}^{4/5} \cdot \bar{M}_I^{\text{exp}}$ [for the definitions see Eqs. (12), (15)] are derived from the current $0\nu\beta\beta$ bounds (1), (2).

eHSM #I	Effective operator decomposition	x, y	C_I^{exp} ^{76}Ge	C_I^{exp} ^{136}Xe	$\bar{M}_I^{\text{exp}}$ TeV ^{76}Ge	$\bar{M}_I^{\text{exp}}$ TeV ^{136}Xe
	$\mathcal{O}^I = x\mathcal{O}_1^{XX} + y\mathcal{O}_2^{XX}$					
1		$-\frac{5}{24}$, $-\frac{1}{32}$	1.4×10^{-9}	6.9×10^{-10}	6.3	7.3
2		$\frac{1}{32}$, $\frac{1}{128}$	9.2×10^{-9}	4.6×10^{-9}	4.3	5.0
3		$-\frac{7}{48}$, $-\frac{1}{192}$	2.0×10^{-9}	9.7×10^{-10}	5.9	6.8
4		$\frac{1}{32}$, $-\frac{1}{128}$	8.9×10^{-9}	4.4×10^{-9}	4.4	5.0
5		$\frac{1}{24}$, $-\frac{1}{96}$	6.7×10^{-9}	3.3×10^{-9}	4.6	5.3
6		$\frac{3}{32}$, $\frac{1}{128}$	3.0×10^{-9}	1.5×10^{-9}	5.4	6.2
	$\mathcal{O}^I = x\mathcal{O}_1^{LR,RL} + y\mathcal{O}_3^{LR,RL}$					
7		$-\frac{1}{12}$, $-\frac{1}{8}$	2.4×10^{-7}	1.2×10^{-7}	2.3	2.6
8		$-\frac{1}{8}$, $-\frac{1}{48}$	6.0×10^{-8}	2.9×10^{-8}	3.0	3.4
9		$\frac{1}{16}$, $\frac{1}{32}$	1.4×10^{-7}	7.0×10^{-8}	2.5	2.9
10		$-\frac{1}{32}$, $\frac{1}{64}$	1.8×10^{-7}	8.9×10^{-8}	2.4	2.7

TABLE III. Continuation of Table II. Experimental limits on the Wilson Coefficients $C_I(\Lambda = 1\ \text{TeV}) \leq C_I^{\text{exp}}$ of these operators and their characteristic scales $M_I \geq \lambda_{\text{eff}}^{4/5} \cdot \bar{M}_I^{\text{exp}}$ [for the definitions see Eqs. (12), (15)] are derived from the current $0\nu\beta\beta$ bounds (1), (2).

eHSM #I	Effective operator decomposition	α, β	C_I^{exp} ^{76}Ge	C_I^{exp} ^{136}Xe	$\bar{M}_I^{\text{exp}}$ TeV ^{76}Ge	$\bar{M}_I^{\text{exp}}$ TeV ^{136}Xe
	$\mathcal{O}^I = x\mathcal{O}_4^{XX} + y\mathcal{O}_5^{XX}$					
11		$-\frac{1}{16i}$, $-\frac{5}{48}$	6.9×10^{-8}	3.5×10^{-8}	2.9	3.3
12		$-\frac{1}{32i}$, $-\frac{1}{32}$	1.2×10^{-7}	6.0×10^{-8}	2.6	3.0
13		$\frac{1}{32i}$, $-\frac{1}{32}$	7.6×10^{-8}	3.9×10^{-8}	2.8	3.2
14		$\frac{1}{48i}$, $\frac{7}{48}$	1.1×10^{-7}	5.5×10^{-8}	2.7	3.0
15		$-\frac{1}{32i}$, $-\frac{3}{32}$	1.6×10^{-7}	8.1×10^{-8}	2.5	2.8
16		$\frac{1}{24i}$, $-\frac{1}{24}$	5.7×10^{-8}	2.9×10^{-8}	3.0	3.4
	$\mathcal{O}^I = x\mathcal{O}_4^{LR,RL} + y\mathcal{O}_5^{LR,RL}$					
17		$\frac{1}{16i}$, $-\frac{5}{48}$	1.5×10^{-7}	7.8×10^{-8}	2.5	2.8
18		$\frac{1}{32i}$, $-\frac{1}{32}$	3.8×10^{-7}	1.9×10^{-7}	2.1	2.4
19		$-\frac{1}{48i}$, $\frac{7}{48}$	1.4×10^{-7}	7.4×10^{-8}	2.5	2.9
20		$\frac{1}{32i}$, $-\frac{3}{32}$	2.0×10^{-7}	1.1×10^{-7}	2.3	2.7
21		$-\frac{1}{32i}$, $-\frac{1}{32}$	3.7×10^{-7}	1.9×10^{-7}	2.1	2.4
22		$-\frac{1}{24i}$, $-\frac{1}{24}$	2.8×10^{-7}	1.4×10^{-7}	2.2	2.5

limits are shown in Tables II, III and IV. For a more direct comparison of the $0\nu\beta\beta$-decay limits with the sensitivity of an accelerator experiment, such as the LHC, it is instructive to convert these limits into limits on the scale M_I of the masses of the intermediate heavy particles mediating the contribution of #I eHSMs to $0\nu\beta\beta$-decay. Denoting the dimensionless couplings in the T-I diagram from Fig. 3 with $\lambda_{1,2,3,4}$ and letting all the intermediate particle masses be of the order of the same scale M_I we can give an estimation

$$\frac{G_F^2}{2m_p} C_I(\Lambda) = \frac{\lambda_1\lambda_2\lambda_3\lambda_4}{M_I^5} \tag{14}$$

for the overall coefficient in Eq. (12). Then we find lower limits for the typical mass scale at which a particular eHSM contributes to the short-range mechanism:

$$M_I \geq \lambda_{\text{eff}}^{4/5} \left(\frac{2m_p}{C_I^{\text{exp}} G_F^2} \right)^{1/5} = \lambda_{\text{eff}}^{4/5} \bar{M}_I^{\text{exp}}, \tag{15}$$

TABLE IV. The same as in Table II, but for eHSMs decomposing in only one of the basis operators Eqs. (4)–(8). Experimental limits on the Wilson Coefficients $C_I(\Lambda = 1\ \text{TeV}) \leq C_I^{\text{exp}}$ of these operators and their characteristic scales $M_I \geq \lambda_{\text{eff}}^{4/5} \cdot \bar{M}_I^{\text{exp}}$ [for the definitions see Eqs. (12), (15)] are derived from the current $0\nu\beta\beta$ bounds (1), (2).

eHSM #I	Effective operator decomposition	C_I^{exp} ^{76}Ge	C_I^{exp} ^{136}Xe	$\bar{M}^{\text{exp}}$ TeV ^{76}Ge	$\bar{M}^{\text{exp}}$ TeV ^{136}Xe
23	$\mathcal{O}^I = \frac{1}{8}\mathcal{O}_1^{XX}$	2.3×10^{-9}	1.1×10^{-9}	5.7	6.6
24	$\mathcal{O}^I = \frac{1}{8}\mathcal{O}_1^{LR,RL}$	5.2×10^{-8}	2.7×10^{-8}	3.0	3.5
25	$\mathcal{O}^I = \frac{1}{32}\mathcal{O}_3^{LR,RL}$	5.0×10^{-7}	2.5×10^{-7}	1.9	2.2
26	$\mathcal{O}^I = \frac{1}{16}\mathcal{O}_5^{XX}$	1.7×10^{-7}	8.5×10^{-8}	2.4	2.8
27	$\mathcal{O}^I = \frac{1}{16}\mathcal{O}_5^{LR}$	3.4×10^{-7}	1.8×10^{-7}	2.1	2.4
28	$\mathcal{O}^I = \frac{1}{16}\mathcal{O}_3^{XX}$	1.9×10^{-7}	9.5×10^{-8}	2.4	2.7

where we introduced for convenience $\lambda_{\text{eff}} = (\lambda_1\lambda_2\lambda_3\lambda_4)^{1/4}$ and C_I^{exp} are the previously derived upper limits on $C_I(\Lambda) \leq C_I^{\text{exp}}$. We show these limits in Tables II–IV for completeness. Note that for T-II diagrams in Fig. 3, the triple-scalar coupling has dimension of mass. Nevertheless, we can apply the same limits, as in the case of T-I, assuming this coupling to be of order $\mu = \lambda_{\text{eff}} M_I$.

Closing this section we emphasize once more the importance of the QCD corrections for some particular short-range HSMs. The largest impact is found for models containing the operator $\mathcal{O}_1^{XX}$. For example, from Table IV one finds a lower limit on $\Lambda_{\text{LNV}} \sim M_I$ of the order $\Lambda_{\text{LNV}} \gtrsim 6.6$ TeV. The corresponding number without QCD corrections would be $\Lambda_{\text{LNV}} \gtrsim 1.8$ TeV. For a detailed comparison of the limits with and without the QCD corrections we refer the reader to Ref. [22].

IV. A NON-TRIVIAL EXAMPLE: R_p SUSY

In the previous section we derived limits on eHSMs. Here, we discuss how to derive limits on models, which contribute with more than one diagram of the type T-I and/or T-II in Fig. 3 to the short-range amplitude of $0\nu\beta\beta$-decay. In terms of the previous section these HSMs are linear combinations of certain eHSMs from the list given in Tables VI–IX. The example we have chosen is the well-known case of R-parity violating supersymmetry (R_pSUSY).

It provides LNV vertices with $\Delta L = 1$ from the superpotential. Importantly, in this model there are the gluino ($\tilde{g}$) and neutralino (χ) Majorana mass terms, originating from the soft SUSY breaking sector. Then R_pSUSY can contribute to a $\Delta L = 2$ process, such as $0\nu\beta\beta$-decay, via the short-range mechanism [30,31] given by Feynman diagrams of the topology T-I in Fig. 3 with two $\Delta L = 1$ vertices, two squarks ($\tilde{q}$) or two selectrons ($\tilde{e}$) and a $\tilde{g}$ or χ in the intermediate state. There are in total three gluino plus six neutralino diagrams Ref. [31], see Fig. 4. It is worth noting that the gluino exchange is known to give the dominant contribution in significant parts of the minimal R_pSUSY parameter space [31]. Below we consider the gluino $\tilde{g}$ and the neutralino χ-exchange contributions separately, as if they were uncorrelated sectors. To make contact with our general method, we first identify the transformation properties of the internal SUSY particles, appearing in the diagram T-I in Fig. 4. The scalars $\tilde{u}_L$ and $\tilde{e}_L$ are members of the $SU(2)_L$ doublets $\tilde{Q}_L$ and $\tilde{L}$, respectively. The SM gauge group assignments of the internal states of the diagrams are then given as: $\tilde{Q}_L = S_{3,2,1/6}$, $\tilde{d}_R = S_{3,1,-1/3}$, $\tilde{L} = S_{1,2,1/2}$, $\tilde{g} = \psi_{8,1,0}$. For the simplicity we consider the case of Bino-dominant lightest neutralino, then $\chi = \psi_{1,1,0}$.

From Tables VI–IX we then identify the operator combination corresponding to each diagram. For the gluino diagrams this results in: diagram (a) corresponds to eHSM #5, (b) to #3 and (c) again to #5. The neutralino diagrams are: (a) and (c) correspond to #4, (b) to #2, while diagrams (d)–(f) can be identified with #23. Note that (d) and (e) come with an additional factor of $-\frac{1}{2}$, see Table VIII.

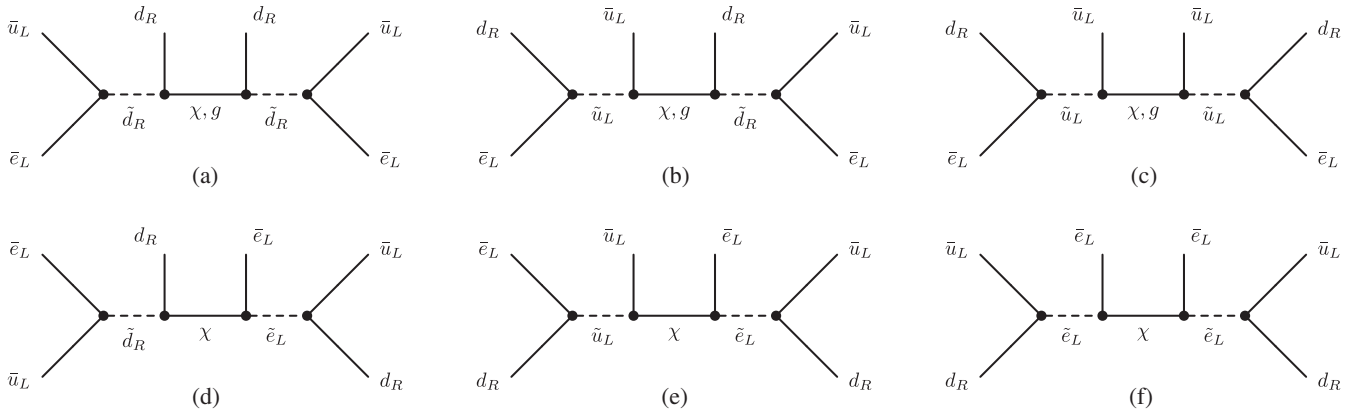

FIG. 4. The six different Feynman diagrams in R-parity violating supersymmetry that contribute to $0\nu\beta\beta$ decay. The diagrams of the gluino $\tilde{g}$ (a), (b), (c) and the neutralino χ (a)-(f) exchange contributions to $0\nu\beta\beta$ decay with the intermediate squarks $\tilde{u}$, $\tilde{d}$ and selectron $\tilde{e}$.

From these considerations, we can reconstruct the corresponding effective Lagrangians in the basis (4)–(8). In this way we find:

$\tilde{g}$-exchange contribution (Fig. 4(a)–(c)):

$$\begin{aligned}\mathcal{L}_{\rm eff}^{\tilde{g}} &= \frac{G_F^2}{2m_p}(C_{\tilde{g}a}\mathcal{O}_a + C_{\tilde{g}b}\mathcal{O}_b + C_{\tilde{g}c}\mathcal{O}_c) \\ &= \frac{G_F^2}{2m_p}\frac{1}{48}\Big[(2C_{\tilde{g}a} + 2C_{\tilde{g}c} - 7C_{\tilde{g}b})\mathcal{O}_1^{RR} \\ &\quad - \frac{1}{4}(2C_{\tilde{g}a} + 2C_{\tilde{g}c} + C_{\tilde{g}b})\mathcal{O}_2^{RR}\Big]. \end{aligned} \tag{16}$$

χ-exchange contribution (Fig. 4(a)–(f)):

$$\begin{aligned}\mathcal{L}_{\rm eff}^{\tilde{g}} &= \frac{G_F^2}{2m_p}\sum_{i=a\cdots f} C_{\#i}\mathcal{O}_{\#i} \\ &= \frac{G_F^2}{2m_p}\frac{1}{128}[4(C_b + C_c + C_a + 4C_f - 2C_d - 2C_e)\mathcal{O}_1^{RR} \\ &\quad + (C_b - C_c - C_a)\mathcal{O}_2^{RR}]. \end{aligned} \tag{17}$$

The Wilson coefficients were calculated in Ref. [31]:

$$C_{\tilde{g}c} = \frac{\kappa_3}{m_{\tilde{g}}}\frac{1}{m_{\tilde{u}_L}^4}, \qquad C_{\tilde{g}a} = \frac{\kappa_3}{m_{\tilde{g}}}\frac{1}{m_{\tilde{d}_R}^4}, \qquad C_{\tilde{g}b} = -\frac{\kappa_3}{m_{\tilde{g}}}\frac{1}{m_{\tilde{u}_L}^2 m_{\tilde{d}_R}^2}, \tag{18}$$

$$C_b = \frac{\kappa_2}{m_\chi}\frac{\epsilon_L(u)\epsilon_R(d)}{m_{\tilde{u}_L}^2 m_{\tilde{d}_R}^2}, \qquad C_c = \frac{\kappa_2}{m_\chi}\frac{\epsilon_L^2(u)}{m_{\tilde{u}_L}^4}, \qquad C_a = \frac{\kappa_2}{m_\chi}\frac{\epsilon_R^2(d)}{m_{\tilde{d}_R}^4}, \tag{19}$$

$$C_f = \frac{\kappa_2}{m_\chi}\frac{\epsilon_L^2(e)}{m_{\tilde{e}_L}^4}, \quad C_d = \frac{\kappa_2}{m_\chi}\frac{\epsilon_L(e)\epsilon_R(d)}{m_{\tilde{e}_L}^2 m_{\tilde{d}_R}^2}, \quad C_e = \frac{\kappa_2}{m_\chi}\frac{\epsilon_L(e)\epsilon_L(u)}{m_{\tilde{e}_L}^2 m_{\tilde{u}_L}^2}, \tag{20}$$

with

$$\kappa_2 = \lambda'^2_{111} 4\pi\alpha_2 \frac{m_p}{G_F^2}, \qquad \kappa_3 = \lambda'^2_{111} 16\pi\alpha_s \frac{m_p}{G_F^2}, \tag{21}$$

$$\epsilon_L(\psi) = \tan\theta_W[T_3(\psi) - Q(\psi)], \qquad \epsilon_R(\psi) = \tan\theta_W Q(\psi), \tag{22}$$

where λ'_{111} is the first generation $\not{R}_p$ SUSY coupling, $\alpha_2 = g_2^2/4\pi$ and $\alpha_s = g_3^2/4\pi$ are the $SU(2)_L$ and $SU(3)_C$ couplings, respectively. As usual G_F is the Fermi constant and m_p is the proton mass. $T_3(\psi)$ and $Q(\psi)$ are the third component of the weak isospin and the electric charge of the fermion ψ.

First we consider the $\tilde{g}$-exchange and derive the limits on the $\not{R}_p$ SUSY parameter space. For this we adopt the conventional assumption $m_{\tilde{u}_L} \approx m_{\tilde{d}_R} \approx m_{\tilde{q}}$. Comparing the Lagrangian (16) with the canonic form (3) and using the half-life formula (10) we find, by taking into account the QCD running, for the current experimental limits (1)–(2) the following upper bounds on the $\not{R}_p$ SUSY Yukawa coupling:

$$\tilde{g}-\text{exchange}:\ \lambda'_{111\text{Ge}} \le 1.0\times10^{-2}\left(\frac{m_{\tilde{q}}}{1\ \text{TeV}}\right)^2\left(\frac{m_{\tilde{g}}}{1\ \text{TeV}}\right)^{1/2}, \tag{23}$$

$$\lambda'_{111Xe} \le 7.2\times10^{-3}\left(\frac{m_{\tilde{q}}}{1\ \text{TeV}}\right)^2\left(\frac{m_{\tilde{g}}}{1\ \text{TeV}}\right)^{1/2} \tag{24}$$

For the case of the neutralino exchange we consider a particular part of the $\not{R}_p$ SUSY parameter space where $m_{\tilde{e}} \ll m_{\tilde{q}}$. This is motivated by the fact that LHC searches set very strong limits on the colored sector of any beyond the SM physics. In this domain the dominant contribution comes from the diagram (f), corresponding to eHSM #23. We find the limits taking into account the QCD running

$$\chi-\text{exchange}:\ \lambda'_{111\text{Ge}} \le 7.3\times10^{-1}\left(\frac{m_{\tilde{e}}}{1\ \text{TeV}}\right)^2\left(\frac{m_{\tilde{\chi}}}{1\ \text{TeV}}\right)^{1/2} \tag{25}$$

$$\lambda'_{111Xe} \le 5.1\times10^{-1}\left(\frac{m_{\tilde{e}}}{1\ \text{TeV}}\right)^2\left(\frac{m_{\tilde{\chi}}}{1\ \text{TeV}}\right)^{1/2} \tag{26}$$

For the calculation of this limit we assumed $N_1 \simeq 1$. Note that the limits from the χ-exchange (25), (26) are competitive with those, which come from the $\tilde{g}$-exchange (23), (24) in the $\not{R}_p$ SUSY parameter space domain $m_{\tilde{q}} \gg m_{\tilde{e}}$ and $m_{\tilde{g}} \gg m_\chi$.

In order to demonstrate the significance of the QCD running we re-calculated the corresponding limit for ^{76}Ge using the same experimental bound (1), but switching off the QCD corrections. This results in a modification of the coefficients β in Table I, which can be found for this limiting case in Ref. [22]. Without QCD running we obtain the limits:

$$\tilde{g}-\text{exchange}:\ \lambda'_{111\text{Ge}} \le 9.3\times10^{-2}\left(\frac{m_{\tilde{q}}}{1\ \text{TeV}}\right)^2\left(\frac{m_{\tilde{g}}}{1\ \text{TeV}}\right)^{1/2}, \tag{27}$$

$$\chi-\text{exchange}:\ \lambda'_{111\text{Ge}} \le 5.2\left(\frac{m_{\tilde{e}}}{1\ \text{TeV}}\right)^2\left(\frac{m_{\tilde{\chi}}}{1\ \text{TeV}}\right)^{1/2} \tag{28}$$

This is about ∼10 (∼7) weaker than the limits for gluino (neutralino) cases in Eqs. (23) and (25) taking into account the QCD running. This again demonstrates the crucial role of the QCD corrections for SRM.

V. DISCUSSIONS AND CONCLUSIONS

In this paper we have calculated QCD-improved lower limits on the Wilson coefficients and the LNV mass scales, $M_I \sim \Lambda_{LNV}$, for all ultraviolet completions ("elementary high-scale models") of the $d = 9$ $0\nu\beta\beta$ decay operator, contributing to the short-range part of the amplitude.

Admittedly, all the limits presented in this paper are subject to NMEs uncertainties, believed to be within a factor 2-3 or so. As seen from the half-life formula (10) and Eqs. (A1)–(A5) the upper limits on the Wilson coefficients C_I are inversely proportional to the NMEs. Therefore, the NMEs uncertainties translate into corresponding factors in the C_I-limits. However, according to Eq. (15) the lower limits on the characteristic eHSM mass scale M_I is significantly weaker, since they scale as $(1/C_I)^{-1/5}$. Limits on M_I, therefore, have uncertainties of order $\sim(2-3)^{1/5}$.

The most crucial impact of the QCD loop corrections is found for the (pseudo-)scalar operators (4), which—due to the color mismatch effect—mix with the tensor operators (4). The key point is that the latter have the NMEs, $\mathcal{M}_2$, much large than the NMEs, $\mathcal{M}_1$, of the (pseudo-)scalar operators. Once QCD corrections are taken into account the large changes in limits on scalar-pseudoscalar operators occur. Let us briefly comment on the huge ratio $\mathcal{M}_2/\mathcal{M}_1$. According to Ref. [15], the (pseudo-)scalar operators lead to a double Fermi type NME, $M_{F,N}$, while the tensor ones to a double Gamow-Teller type NME, $M_{GT,N}$. In the QRPA calculations, $M_{GT,N}/M_{F,N}$ is typically of order $\mathcal{O}(3)$. However, the hadronization of the (pseudo-)scalar quark currents to nucleon currents introduce a much smaller normalization constant than in the case of the tensor currents, as seen from Eq. (8) of Ref. [15]. The ratio of the prefactors α_2/α_1, calculated with the values of the scalar and tensor nucleon form factors from Refs. [32,33], is roughly $\mathcal{O}(60)$. Thus the large value of $\mathcal{M}_2/\mathcal{M}_1$ comes essentially from the hadronization of the quark currents and is not a nuclear structure effect.

In closing, we have worked out a general method, which can be used for finding the limits for any particular high-scale model, contributing to the SRM of $0\nu\beta\beta$ decay with several diagrams. Our method can be used to find new, improved limits easily, should better experimental limits or new calculations of the nuclear matrix elements become available. We would like to stress again, that QCD running can lead to important changes in the $0\nu\beta\beta$ decay limits on the mass scales of LNV extensions of the SM.

ACKNOWLEDGMENTS

Marcela and Carolina are grateful for the hospitality of the AHEP group in the IFIC during their visits. This work was supported by the Spanish MICINN Grants No. SEV-2014-0398, No. FPA2014-58183-P and Multidark CSD2009-00064 (MINECO), and PROMETEOII/2014/084 (Generalitat Valenciana), and by Fondecyt (Chile) under Grants No. 3150472, No. 1150792 and No. 3160642 as well as CONICYT (Chile) Ring ACT 1406 and CONICYT PIA/Basal FB0821. M. H. thanks the Universidad Técnica Federico Santa María, Valparaíso, for hospitality.

APPENDIX A: β-PARAMETERS OF HALF-LIFE FORMULA

The coefficients β entering into the $0\nu\beta\beta$-decay half-life formula (10) are given by [22]:

$$\beta_1^{XX} = \mathcal{M}_1 U^{XX}_{(12)11} + \mathcal{M}_2 U^{XX}_{(12)21},$$
$$\beta_1^{LR} = \mathcal{M}_3^{(+)} U^{LR}_{(31)12} + \mathcal{M}_1 U^{LR}_{(31)22}, \tag{A1}$$

$$\beta_2^{XX} = \mathcal{M}_1 U^{XX}_{(12)12} + \mathcal{M}_2 U^{XX}_{(12)22}, \tag{A2}$$

$$\beta_3^{XX} = \mathcal{M}_3^{(-)} U^{XX}_{(3)}, \qquad \beta_3^{LR} = \mathcal{M}_3^{(+)} U^{LR}_{(31)11} \tag{A3}$$

$$\beta_4^{XX} = -|\mathcal{M}_4| U^{XX}_{(45)11} + |\mathcal{M}_5| U^{XX}_{(45)21}, \qquad \beta_4^{LR} = |\mathcal{M}_4| U^{LR}_{(4)}, \tag{A4}$$

$$\beta_5^{XX} = -|\mathcal{M}_4| U^{XX}_{(45)12} + |\mathcal{M}_5| U^{XX}_{(45)22}, \qquad \beta_5^{LR} = |\mathcal{M}_5| U^{LR}_{(5)}. \tag{A5}$$

The subscripts of the RGE μ-evolution matrix U in the parenthesis denote the subscripts of the operators from Eqs. (4)–(8) mixed under the renormalization, the subscripts without the parenthesis specify the U-matrix element. Numerical values of these matrix elements, properly taking into account the quark thresholds, are

$$\hat{U}^{XX}_{(12)}(\mu_0, \Lambda_1) = \begin{pmatrix} 1.88 & 0.06 \\ -2.76 & 0.40 \end{pmatrix}, \qquad U^{XX}_{(3)}(\mu_0, \Lambda_1) = 0.76, \tag{A6}$$

$$\hat{U}^{LR}_{(31)}(\mu_0, \Lambda_1) = \begin{pmatrix} 0.87 & -1.40 \\ 0 & 2.97 \end{pmatrix},$$
$$\hat{U}^{XX}_{(45)}(\mu_0, \Lambda_1) = \begin{pmatrix} 2.33 & 0.39i \\ 0.64i & 3.35 \end{pmatrix}, \tag{A7}$$

$$U^{LR}_{(4)}(\mu_0, \Lambda_1) = 0.70, \qquad U^{LR}_{(5)}(\mu_0, \Lambda_1) = 2.97. \tag{A8}$$

and

TABLE V. The numerical values of the nuclear matrix elements $\mathcal{M}_i$ taken from Ref. [2].

${}^AX$	$\mathcal{M}_1$	$\mathcal{M}_2$	$\mathcal{M}_3^{(+)}$	$\mathcal{M}_3^{(-)}$	$\lvert\mathcal{M}_4\rvert$	$\lvert\mathcal{M}_5\rvert$
^{76}Ge	9.0	-1.6×10^3	1.3×10^2	2.1×10^2	$\lvert1.9\times10^2\rvert$	$\lvert1.9\times10^1\rvert$
^{136}Xe	4.5	-8.5×10^2	6.9×10^1	1.1×10^2	$\lvert9.6\times10^1\rvert$	$\lvert9.3\rvert$

$$\hat{U}^{XX}_{(12)}(\mu_0,\Lambda_2)=\begin{pmatrix}2.24 & 0.07\\ -3.70 & 0.27\end{pmatrix},$$
$$U^{XX}_{(3)}(\mu_0,\Lambda_2)=0.70, \tag{A9}$$

$$\hat{U}^{LR}_{(31)}(\mu_0,\Lambda_2)=\begin{pmatrix}0.84 & -2.19\\ 0 & 4.13\end{pmatrix},$$
$$\hat{U}^{XX}_{(45)}(\mu_0,\Lambda_2)=\begin{pmatrix}2.98 & 0.69i\\ 1.15i & 4.82\end{pmatrix}, \tag{A10}$$

$$U^{LR}_{(4)}(\mu_0,\Lambda_2)=0.62,\qquad U^{LR}_{(5)}(\mu_0,\Lambda_2)=4.13. \tag{A11}$$

for two reference values, $\Lambda_1=M_W$ and $\Lambda_2=1$ TeV, of the high energy scale Λ, and $\mu_0=1$ Gev for the low energy one.

Using Eqs. (A1)–(A11) one can calculate the numerical values of the β_i^{XY}-coefficients (A1)–(A5) for the NMEs derived in a particular model of nuclear structure. The values given in Table I have been calculated with the NMEs $\mathcal{M}_i$ taken from Ref. [2] and displayed in Table V.

APPENDIX B: SPECIFICATION OF eHSMs AND NOTATIONS

Here we comment on the notations used in Tables VI–IX where we specify all the eHSMs contributing to $0\nu\beta\beta$-decay via the short-range mechanism according to T-I and T-II diagrams in Fig. 3 with heavy intermediate particles (messengers). Each eHSM is uniquely specified by the SM gauge group $G_{\rm SM}=SU(3)_c\times SU(2)_L\times U(1)_Y$ assignments of the messengers: Scalar-Fermion-Scalar $\{(S),(\psi),(S')\}$ for diagram T-I and triple scalar $\{(S),(S'),(S'')\}$ for T-II. Thus each set of $G_{\rm SM}$ representations in curled brackets corresponds to a particular eHSM $=\{(),(),()\}$. The list of the models is taken from Ref. [26], however, in our tables we put the eHSMs in groups with an identifier #I. The eHSMs from the same group lead in the low-energy limit after integrating out the heavy particles to the same effective operator $\mathcal{O}^I$. These operators in the form (11) are given in Tables II–IV.

Some eHSMs appear in Tables VI–IX with numerical coefficients α, like $\alpha\cdot\{(),(),()\}$. In our notations this means that in the low-energy limit the models belonging to the group #I tend to the same effective operator $\mathcal{O}^I$ but with different normalization factors so that

$$\left.\begin{matrix}\alpha\cdot\{(),(),()\}\\ \{(),(),()\}\end{matrix}\right\}\to\mathcal{O}^I \tag{B1}$$

For example, in the group #1 we find the eHSMs for which

$$-2\cdot\{(),(),()\}:\ \{(\mathbf{8},\mathbf{2};1/2),(\bar{\mathbf{3}},\mathbf{2};5/6),(\bar{\mathbf{3}},\mathbf{1};1/3)\}\to-\frac{1}{2}\cdot\mathcal{O}^{I=1} \tag{B2}$$

$$\{(),(),()\}:\ \{(\mathbf{8},\mathbf{2};1/2),(\mathbf{8},\mathbf{1};0),(\mathbf{8},\mathbf{2};-1/2)\}\to\mathcal{O}^{I=1} \tag{B3}$$

We also used a shorthand notation for the subsets of eHSMs in a particular group #I inside the blue boldface curled brackets, which means

$$\alpha\cdot\{\{(),(),()\},\ldots,\{(),(),()\}\ldots\}=\alpha\cdot\{(),(),()\},\ldots,\alpha\cdot\{(),(),()\}\ldots \tag{B4}$$

Limits on the Wilson coefficients C_I of the eHSMs and their characteristic mass scales M_I are given in Tables II–IV for each eHSM listed in Tables VI–IX. For an eHSM appearing in the latter Tables with a numerical coefficient eHSM $=\alpha\cdot\{(),(),()\}$ the upper limit from Tables II–IV on its Wilson coefficient should be replaced with $\alpha\cdot C_I^{\rm exp}$ and the lower limit on the mass scale with $\alpha^{-1/5}\bar{M}_I^{\rm exp}$.

We refer the reader to Ref. [26] for the detailed rules of the reconstruction of the operators $\mathcal{O}^I$ starting from the eHSM messenger assignment $\{(),(),()\}$ given in Tables VI–IX.

TABLE VI. Identification of the T-I (Fig. 3) short-range eHSMs. For explanation of notations see Appendix B and the main text.

eHSM #I	T-I Mediators $(SU(3)_c, SU(2)_L, U(1)_Y)$ with $Y = Q - T_3$ $\{(S), (\psi), (S')\}$
1	$\{(\mathbf{8},\mathbf{2};1/2),(\mathbf{8},\mathbf{1};0),(\mathbf{8},\mathbf{2};-1/2)\},\{(\mathbf{8},\mathbf{2};1/2),(\mathbf{8},\mathbf{3};0),(\mathbf{8},\mathbf{2};-1/2)\},\{(\mathbf{8},\mathbf{2};1/2),(\mathbf{3},\mathbf{3};2/3),(\mathbf{1},\mathbf{3};1)\},$ $\{(\mathbf{8},\mathbf{2};1/2),(\mathbf{3},\mathbf{2};7/6),(\mathbf{1},\mathbf{3};1)\},\{(\mathbf{8},\mathbf{2};1/2),(\bar{\mathbf{3}},\mathbf{2};5/6),(\mathbf{1},\mathbf{3};1)\},\{(\mathbf{8},\mathbf{2};1/2),(\bar{\mathbf{3}},\mathbf{3};1/3),(\mathbf{1},\mathbf{3};1)\}$ $-2\cdot\{\{(\mathbf{8},\mathbf{2};1/2),(\bar{\mathbf{3}},\mathbf{2};5/6),(\bar{\mathbf{3}},\mathbf{1};1/3)\},\{(\mathbf{8},\mathbf{2};1/2),(\bar{\mathbf{3}},\mathbf{2};5/6),(\bar{\mathbf{3}},\mathbf{3};1/3)\},\{(\mathbf{8},\mathbf{2};1/2),(\mathbf{8},\mathbf{1};0),(\bar{\mathbf{3}},\mathbf{1};1/3)\},$ $\{(\mathbf{8},\mathbf{2};1/2),(\mathbf{8},\mathbf{3};0),(\bar{\mathbf{3}},\mathbf{3};1/3)\},\{(\mathbf{8},\mathbf{2};1/2),(\mathbf{3},\mathbf{3};2/3),(\mathbf{3},\mathbf{2};1/6)\},\{(\mathbf{8},\mathbf{2};1/2),(\mathbf{8},\mathbf{1};0),(\mathbf{3},\mathbf{2};1/6)\}$ $\{(\mathbf{8},\mathbf{2};1/2),(\mathbf{8},\mathbf{3};0),(\mathbf{3},\mathbf{2};1/6)\}\}$
2	$\{(\bar{\mathbf{3}},\mathbf{2};-1/6),(\mathbf{1},\mathbf{1};0),(\bar{\mathbf{3}},\mathbf{1};1/3)\},\{(\bar{\mathbf{3}},\mathbf{2};-1/6),(\mathbf{1},\mathbf{3};0),(\bar{\mathbf{3}},\mathbf{3};1/3)\}$
3	$\{(\bar{\mathbf{3}},\mathbf{2};-1/6),(\mathbf{8},\mathbf{1};0),(\bar{\mathbf{3}},\mathbf{1};1/3)\},\{(\bar{\mathbf{3}},\mathbf{2};-1/6),(\mathbf{8},\mathbf{3};0),(\bar{\mathbf{3}},\mathbf{3};1/3)\}$
4	$\{(\bar{\mathbf{3}},\mathbf{2};-1/6),(\mathbf{1},\mathbf{1};0),(\mathbf{3},\mathbf{2};1/6)\},\{(\bar{\mathbf{3}},\mathbf{2};-1/6),(\mathbf{1},\mathbf{3};0),(\mathbf{3},\mathbf{2};1/6)\},\{(\mathbf{6},\mathbf{3};1/3),(\mathbf{3},\mathbf{3};2/3),(\mathbf{3},\mathbf{2};1/6)\},$ $\{(\mathbf{6},\mathbf{3};1/3),(\mathbf{6},\mathbf{2};-1/6),(\mathbf{3},\mathbf{2};1/6)\},\{(\mathbf{3},\mathbf{1};-1/3),(\mathbf{1},\mathbf{1};0),(\bar{\mathbf{3}},\mathbf{1};1/3)\},\{(\mathbf{3},\mathbf{3};-1/3),(\mathbf{1},\mathbf{3};0),(\bar{\mathbf{3}},\mathbf{3};1/3)\}$ $\{(\mathbf{3},\mathbf{1};-1/3),(\mathbf{6},\mathbf{2};-1/6),(\mathbf{6},\mathbf{1};-2/3)\},\{(\mathbf{3},\mathbf{3};-1/3),(\mathbf{6},\mathbf{2};-1/6),(\mathbf{6},\mathbf{1};-2/3)\},\{(\mathbf{3},\mathbf{1};-1/3),(\mathbf{3},\mathbf{2};-5/6),(\mathbf{6},\mathbf{1};-2/3)\}$ $\{(\mathbf{3},\mathbf{3};-1/3),(\mathbf{3},\mathbf{2};-5/6),(\mathbf{6},\mathbf{1};-2/3)\}$ $-2\cdot\{\{(\bar{\mathbf{3}},\mathbf{2};-1/6),(\bar{\mathbf{6}},\mathbf{2};1/6),(\bar{\mathbf{3}},\mathbf{1};1/3)\},\{(\bar{\mathbf{3}},\mathbf{2};-1/6),(\bar{\mathbf{6}},\mathbf{2};1/6),(\bar{\mathbf{3}},\mathbf{3};1/3)\}\}$ $-\frac{1}{2}\cdot\{\{(\mathbf{6},\mathbf{3};1/3),(\mathbf{6},\mathbf{2};-1/6),(\mathbf{6},\mathbf{1};-2/3)\},\{(\mathbf{6},\mathbf{1};4/3),(\mathbf{6},\mathbf{2};5/6),(\mathbf{6},\mathbf{3};1/3)\},\{(\mathbf{6},\mathbf{3};1/3),(\mathbf{3},\mathbf{3};2/3),(\mathbf{1},\mathbf{3};1),\}$ $\{(\mathbf{6},\mathbf{1};4/3),(\mathbf{3},\mathbf{2};7/6),(\mathbf{1},\mathbf{3};1)\},\{(\bar{\mathbf{6}},\mathbf{3};-1/3),(\bar{\mathbf{3}},\mathbf{3};1/3),(\mathbf{1},\mathbf{3};1)\},\{(\bar{\mathbf{6}},\mathbf{1};2/3),(\bar{\mathbf{3}},\mathbf{2};5/6),(\mathbf{1},\mathbf{3};1)\}\}$
5	$\{(\bar{\mathbf{3}},\mathbf{2};-1/6),(\mathbf{8},\mathbf{1};0),(\mathbf{3},\mathbf{2};1/6)\},\{(\bar{\mathbf{3}},\mathbf{2};-1/6),(\mathbf{8},\mathbf{3};0),(\mathbf{3},\mathbf{2};1/6)\},\{(\mathbf{3},\mathbf{1};-1/3),(\mathbf{8},\mathbf{1};0),(\bar{\mathbf{3}},\mathbf{1};1/3)\}$ $\{(\mathbf{3},\mathbf{3};-1/3),(\mathbf{1},\mathbf{3};0),(\bar{\mathbf{3}},\mathbf{3};1/3)\}$
6	$\{(\bar{\mathbf{3}},\mathbf{2};-1/6),(\mathbf{3},\mathbf{2};1/6),(\bar{\mathbf{3}},\mathbf{1};1/3)\},\{(\bar{\mathbf{3}},\mathbf{2};-1/6),(\mathbf{3},\mathbf{2};1/6),(\bar{\mathbf{3}},\mathbf{3};1/3)\}$
7	$\{(\mathbf{8},\mathbf{2};1/2),(\mathbf{8},\mathbf{1};0),(\mathbf{8},\mathbf{2};-1/2)\},\{(\mathbf{8},\mathbf{2};1/2),(\mathbf{8},\mathbf{3};0),(\mathbf{8},\mathbf{2};-1/2)\},\{(\mathbf{8},\mathbf{2};1/2),(\mathbf{3},\mathbf{2};7/6),(\mathbf{1},\mathbf{3};1)\},$ $\{(\mathbf{8},\mathbf{2};1/2),(\mathbf{3},\mathbf{3};2/3),(\mathbf{1},\mathbf{3};1)\},\{(\mathbf{8},\mathbf{2};1/2),(\bar{\mathbf{3}},\mathbf{3};1/3),(\mathbf{1},\mathbf{3};1)\},\{(\mathbf{8},\mathbf{2};1/2),(\bar{\mathbf{3}},\mathbf{2};5/6),(\mathbf{1},\mathbf{3};1)\}$ $-2\cdot\{\{(\mathbf{8},\mathbf{2};1/2),(\bar{\mathbf{3}},\mathbf{2};5/6),(\bar{\mathbf{3}},\mathbf{1};1/3)\},\{(\mathbf{8},\mathbf{2};1/2),(\bar{\mathbf{3}},\mathbf{2};5/6),(\bar{\mathbf{3}},\mathbf{3};1/3)\},\{(\mathbf{8},\mathbf{2};1/2),(\mathbf{8},\mathbf{1};0)(\bar{\mathbf{3}},\mathbf{1};1/3)\},$ $\{(\mathbf{8},\mathbf{2};1/2),(\mathbf{8},\mathbf{3};0),(\bar{\mathbf{3}},\mathbf{3};1/3)\},\{(\mathbf{8},\mathbf{2};1/2),(\mathbf{3},\mathbf{3};2/3),(\mathbf{3},\mathbf{2};1/6)\},\{(\mathbf{8},\mathbf{2};1/2),(\mathbf{8},\mathbf{1};0),(\mathbf{3},\mathbf{2};1/6)\},$ $\{(\mathbf{8},\mathbf{2};1/2),(\mathbf{8},\mathbf{3};0),(\mathbf{3},\mathbf{2};1/6)\}\}$

TABLE VII. Continuation of Table VI.

eHSM #I	T-I Mediators $(SU(3)_c, SU(2)_L, U(1)_Y)$ with $Y = Q - T_3$ $\{(S), (\psi), S'\}$
8	$\{(\bar{\mathbf{3}},\mathbf{2};-1/6),(\mathbf{8},\mathbf{2};1/2),(\bar{\mathbf{3}},\mathbf{1};1/3)\},\{(\bar{\mathbf{3}},\mathbf{2};-1/6),(\mathbf{8},\mathbf{2};1/2),(\bar{\mathbf{3}},\mathbf{3};1/3)$
9	$\{(\bar{\mathbf{3}},\mathbf{2};-1/6),(\mathbf{3},\mathbf{1};-1/3),(\bar{\mathbf{3}},\mathbf{1};1/3)\},\{(\bar{\mathbf{3}},\mathbf{2};-1/6),(\mathbf{3},\mathbf{3};-1/3),(\bar{\mathbf{3}},\mathbf{3};1/3)\}$
10	$\{(\bar{\mathbf{3}},\mathbf{2};-1/6),(\bar{\mathbf{6}},\mathbf{1};-1/3),(\bar{\mathbf{3}},\mathbf{1};1/3)\},\{(\bar{\mathbf{3}},\mathbf{2};-1/6),(\bar{\mathbf{6}},\mathbf{3};-1/3),(\bar{\mathbf{3}},\mathbf{3};1/3)\}$
11	$\{(\mathbf{8},\mathbf{2};1/2),(\bar{\mathbf{3}},\mathbf{2};5/6),(\bar{\mathbf{3}},\mathbf{1};1/3)\},\{(\mathbf{8},\mathbf{2};1/2),(\mathbf{8},\mathbf{1};0),(\bar{\mathbf{3}},\mathbf{1};1/3)\},\{(\mathbf{8},\mathbf{2};1/2),(\mathbf{3},\mathbf{2};7/6),(\mathbf{3},\mathbf{2};1/6)\}$ $\{(\mathbf{8},\mathbf{2};1/2),(\mathbf{8},\mathbf{2};-1/2),(\mathbf{3},\mathbf{2};1/6)\}$
12	$\{(\bar{\mathbf{3}},\mathbf{2};-1/6),(\mathbf{1},\mathbf{1};0),(\bar{\mathbf{3}},\mathbf{1};1/3)\}$
13	$\{(\mathbf{3},\mathbf{1};-1/3),(\mathbf{1},\mathbf{1};0),(\bar{\mathbf{3}},\mathbf{1};1/3)\},\{(\mathbf{3},\mathbf{1};-1/3),(\mathbf{6},\mathbf{1};1/3),(\mathbf{6},\mathbf{1};-2/3)\},\{(\mathbf{3},\mathbf{1};-1/3),(\mathbf{6},\mathbf{2};-1/6),(\mathbf{6},\mathbf{1};-2/3)\}$ $\{(\mathbf{3},\mathbf{1};-1/3),(\mathbf{3},\mathbf{1};-4/3),(\mathbf{6},\mathbf{1};-2/3)\},\{(\mathbf{3},\mathbf{1};-1/3),(\mathbf{3},\mathbf{2};-5/6),(\mathbf{6},\mathbf{1};-2/3)\}$ $-2\cdot\{\{(\bar{\mathbf{3}},\mathbf{2};-1/6),(\bar{\mathbf{6}},\mathbf{2};1/6),(\bar{\mathbf{3}},\mathbf{1};1/3)\}\}$
14	$\{(\bar{\mathbf{3}},\mathbf{2};-1/6),(\mathbf{8},\mathbf{1};0),(\bar{\mathbf{3}},\mathbf{1};1/3)\}$
15	$\{(\bar{\mathbf{3}},\mathbf{2};-1/6),(\mathbf{3},\mathbf{2};1/6),(\bar{\mathbf{3}},\mathbf{1};1/3)\}$
16	$\{(\mathbf{3},\mathbf{1};-1/3),(\mathbf{8},\mathbf{1};0),(\bar{\mathbf{3}},\mathbf{1};1/3)\}$
17	$\{(\mathbf{8},\mathbf{2};1/2),(\bar{\mathbf{3}},\mathbf{2};5/6),(\bar{\mathbf{3}},\mathbf{1};1/3)\},\{(\mathbf{8},\mathbf{2};1/2),(\mathbf{8},\mathbf{1};0),(\bar{\mathbf{3}},\mathbf{1};1/3)\},\{(\mathbf{8},\mathbf{2};1/2),(\mathbf{3},\mathbf{2};7/6),(\mathbf{3},\mathbf{2};1/6)\}$ $\{(\mathbf{8},\mathbf{2};1/2),(\mathbf{8},\mathbf{2};-1/2),(\mathbf{3},\mathbf{2};1/6)\}$
18	$\{(\bar{\mathbf{3}},\mathbf{2};-1/6),(\mathbf{1},\mathbf{2};1/2),(\bar{\mathbf{3}},\mathbf{1};1/3)\}$
19	$\{(\bar{\mathbf{3}},\mathbf{2};-1/6),(\mathbf{8},\mathbf{2};1/2),(\bar{\mathbf{3}},\mathbf{1};1/3)\}$ $\{(\bar{\mathbf{3}},\mathbf{2};-1/6),(\mathbf{8},\mathbf{1};0),(\bar{\mathbf{3}},\mathbf{1};1/3)\}$
20	$\{(\bar{\mathbf{3}},\mathbf{2};-1/6),(\mathbf{3},\mathbf{1};-1/3),(\bar{\mathbf{3}},\mathbf{1};1/3)\}$

TABLE VIII. Continuation of Table VI.

eHSM #I	T-I Mediators $(SU(3)_c, SU(2)_L, U(1)_Y)$ with $Y = Q - T_3$ $\{(S), (\psi), (S')\}$
21	$\{(\bar{\mathbf{3}}, \mathbf{2}; -7/6), (\mathbf{1}, \mathbf{2}; -1/2), (\mathbf{3}, \mathbf{2}; 1/6)\}, \{(\mathbf{6}, \mathbf{1}; 4/3), (\mathbf{3}, \mathbf{2}; 7/6), (\mathbf{3}, \mathbf{2}; 1/6)\}, \{(\mathbf{6}, \mathbf{1}; 4/3), (\mathbf{3}, \mathbf{1}; 5/3), (\mathbf{3}, \mathbf{2}; 7/6)\}$ $\{(\mathbf{6}, \mathbf{1}; 4/3), (\mathbf{6}, \mathbf{1}; 1/3), (\mathbf{3}, \mathbf{2}; 1/6)\}, \{(\mathbf{6}, \mathbf{1}; 4/3), (\mathbf{6}, \mathbf{2}; 5/6), (\mathbf{3}, \mathbf{2}; 7/6)\},$ $-2 \cdot \{\{(\bar{\mathbf{3}}, \mathbf{2}; -1/6), (\bar{\mathbf{6}}, \mathbf{1}; -1/3), (\bar{\mathbf{3}}, \mathbf{1}; 1/3)\}\}$
22	$\{(\bar{\mathbf{3}}, \mathbf{2}; -7/6), (\mathbf{8}, \mathbf{2}; -1/2), (\mathbf{3}, \mathbf{2}; 1/6)\}$
23	$\{(\mathbf{1}, \mathbf{2}; 1/2), (\mathbf{1}, \mathbf{1}; 0), (\mathbf{1}, \mathbf{2}; 1/2)\}, \{(\mathbf{1}, \mathbf{2}; 1/2), (\mathbf{1}, \mathbf{3}; 0), (\mathbf{1}, \mathbf{2}; -1/2)\}, \{(\mathbf{1}, \mathbf{2}; 1/2), (\mathbf{3}, \mathbf{3}; 2/3), (\bar{\mathbf{1}}, \mathbf{3}; 1)\},$ $\{(\mathbf{1}, \mathbf{2}; 1/2), (\bar{\mathbf{3}}, \mathbf{2}; 7/6), (\mathbf{1}, \mathbf{3}; 1)\}, \{(\mathbf{1}, \mathbf{2}; 1/2), (\bar{\mathbf{3}}, \mathbf{2}; 5/6), (\mathbf{1}, \mathbf{3}; 1)\}, \{(\mathbf{1}, \mathbf{2}; 1/2), (\bar{\mathbf{3}}, \mathbf{3}; 1/3), (\mathbf{1}, \mathbf{3}; 1)\}$ $-2 \cdot \{\{(\mathbf{1}, \mathbf{2}; 1/2), (\bar{\mathbf{3}}, \mathbf{2}; 5/6), (\bar{\mathbf{3}}, \mathbf{1}; 1/3)\}, \{(\mathbf{1}, \mathbf{2}; 1/2), (\bar{\mathbf{3}}, \mathbf{2}; 5/6), (\bar{\mathbf{3}}, \mathbf{3}; 1/3)\}, \{(\mathbf{1}, \mathbf{2}; 1/2), (\mathbf{1}, \mathbf{1}; 0), (\bar{\mathbf{3}}, \mathbf{1}; 1/3)\},$ $\{(\mathbf{1}, \mathbf{2}; 1/2), (\mathbf{1}, \mathbf{3}; 0), (\bar{\mathbf{3}}, \mathbf{3}; 1/3)\}, \{(\mathbf{1}, \mathbf{2}; 1/2), (\mathbf{3}, \mathbf{3}; 2/3), (\mathbf{3}, \mathbf{2}; 1/6)\}, \{(\mathbf{1}, \mathbf{2}; 1/2), (\mathbf{1}, \mathbf{1}; 0), (\mathbf{3}, \mathbf{2}; 1/6)\},$ $\{(\mathbf{1}, \mathbf{2}; 1/2), (\mathbf{1}, \mathbf{3}; 0), (\mathbf{3}, \mathbf{2}; 1/6)\}\}$
24	$\{(\mathbf{1}, \mathbf{2}; 1/2), (\mathbf{1}, \mathbf{1}; 0), (\mathbf{1}, \mathbf{2}; -1/2)\}, \{(\mathbf{1}, \mathbf{2}; 1/2), (\mathbf{1}, \mathbf{3}; 0), (\mathbf{1}, \mathbf{2}; -1/2)\}, \{(\mathbf{1}, \mathbf{2}; 1/2), (\mathbf{3}, \mathbf{2}; 7/6), (\mathbf{1}, \mathbf{3}; 1)\},$ $\{(\mathbf{1}, \mathbf{2}; 1/2), (\mathbf{3}, \mathbf{3}; 2/3), (\mathbf{1}, \mathbf{3}; 1)\}, \{(\mathbf{1}, \mathbf{2}; 1/2), (\bar{\mathbf{3}}, \mathbf{3}; 1/3), (\mathbf{1}, \mathbf{3}; 1)\}, \{(\mathbf{1}, \mathbf{2}; 1/2), (\bar{\mathbf{3}}, \mathbf{2}; 5/6), (\mathbf{1}, \mathbf{3}; 1)\}$ $-2 \cdot \{\{(\mathbf{1}, \mathbf{2}; 1/2), (\bar{\mathbf{3}}, \mathbf{2}; 5/6), (\bar{\mathbf{3}}, \mathbf{1}; 1/3)\}, \{(\mathbf{1}, \mathbf{2}; 1/2), (\bar{\mathbf{3}}, \mathbf{2}; 5/6), (\bar{\mathbf{3}}, \mathbf{3}; 1/3)\}, \{(\mathbf{1}, \mathbf{2}; 1/2), (\mathbf{1}, \mathbf{1}; 0), (\bar{\mathbf{3}}, \mathbf{1}; 1/3)\},$ $\{(\mathbf{1}, \mathbf{2}; 1/2), (\mathbf{1}, \mathbf{3}; 0), (\bar{\mathbf{3}}, \mathbf{3}; 1/3)\}, \{(\mathbf{1}, \mathbf{2}; 1/2), (\mathbf{3}, \mathbf{3}; 2/3), (\mathbf{3}, \mathbf{2}; 1/6)\}, \{(\mathbf{1}, \mathbf{2}; 1/2), (\mathbf{1}, \mathbf{1}; 0), (\mathbf{3}, \mathbf{2}; 1/6)\},$ $\{(\mathbf{1}, \mathbf{2}; 1/2), (\mathbf{1}, \mathbf{3}; 0), (\mathbf{3}, \mathbf{2}; 1/6)\}\}$
25	$\{(\bar{\mathbf{3}}, \mathbf{2}; -1/6), (\mathbf{1}, \mathbf{2}; 1/2), (\bar{\mathbf{3}}, \mathbf{1}; 1/3)\}, \{(\bar{\mathbf{3}}, \mathbf{2}; -1/6), (\mathbf{1}, \mathbf{2}; 1/2), (\bar{\mathbf{3}}, \mathbf{3}; 1/3)\}$
26	$\{(\mathbf{1}, \mathbf{2}; 1/2), (\bar{\mathbf{3}}, \mathbf{2}; 5/6), (\bar{\mathbf{3}}, \mathbf{1}; 1/3)\}, \{(\mathbf{1}, \mathbf{2}; 1/2), (\mathbf{1}, \mathbf{1}; 0), (\bar{\mathbf{3}}, \mathbf{1}; 1/3)\}, \{(\mathbf{1}, \mathbf{2}; 1/2), (\mathbf{3}, \mathbf{2}; 7/6), (\mathbf{3}, \mathbf{2}; 1/6)\},$ $\{(\mathbf{1}, \mathbf{2}; 1/2), (\mathbf{1}, \mathbf{2}; -1/2), (\bar{\mathbf{3}}, \mathbf{2}; 1/6)\}\}$
27	$\{(\mathbf{1}, \mathbf{2}; 1/2), (\bar{\mathbf{3}}, \mathbf{2}; 5/6), (\bar{\mathbf{3}}, \mathbf{1}; 1/3)\}, \{(\mathbf{1}, \mathbf{2}; 1/2), (\mathbf{1}, \mathbf{1}; 0), (\bar{\mathbf{3}}, \mathbf{1}; 1/3)\}, \{(\mathbf{1}, \mathbf{2}; 1/2), (\mathbf{3}, \mathbf{2}; 7/6), (\mathbf{3}, \mathbf{2}; 1/6)\},$ $\{(\mathbf{1}, \mathbf{2}; 1/2), (\mathbf{1}, \mathbf{2}; -1/2), (\mathbf{3}, \mathbf{2}; 1/6)\}\}$
28	$\{(\mathbf{6}, \mathbf{1}; 4/3), (\mathbf{6}, \mathbf{1}; 1/3), (\mathbf{6}, \mathbf{1}; -2/3)\}, \{(\mathbf{6}, \mathbf{1}; 4/3), (\mathbf{3}, \mathbf{1}; 5/3), (\mathbf{1}, \mathbf{1}; 2)\}, \{(\bar{\mathbf{6}}, \mathbf{1}; 2/3), (\bar{\mathbf{3}}, \mathbf{1}; 4/3), (\mathbf{1}, \mathbf{1}; 2\},$ $-2 \cdot \{(\mathbf{3}, \mathbf{1}; -1/3), (\mathbf{1}, \mathbf{1}; 0), (\bar{\mathbf{3}}, \mathbf{1}; 1/3)\}, \{(\mathbf{3}, \mathbf{1}; -1/3), (\mathbf{6}, \mathbf{1}; 1/3), (\mathbf{6}, \mathbf{1}; -2/3)\}, \{(\mathbf{3}, \mathbf{1}; -1/3), (\mathbf{3}, \mathbf{1}; -4/3), (\mathbf{6}, \mathbf{1}; -2/3\}\}$ $-\frac{3}{2} \cdot \{(\mathbf{3}, \mathbf{1}; -1/3), (\mathbf{8}, \mathbf{1}; 0), (\bar{\mathbf{3}}, \mathbf{1}; 1/3)\}\}$

TABLE IX. Identification of the T-II short-range eHSMs. For notations see Appendix and the main text.

eHSM #I	T-II Mediators $(SU(3)_c, SU(2)_L, U(1)_Y)$ with $Y = Q - T_3$ $\{(S), (S'), (S'')\}$
1	$\{(\mathbf{8}, \mathbf{2}; 1/2), (\mathbf{8}, \mathbf{2}; 1/2), (\mathbf{1}, \mathbf{3}; -1)\}$ $-2 \cdot \{\{(\mathbf{8}, \mathbf{2}; 1/2), (\mathbf{3}, \mathbf{1}; -1/3), (\bar{\mathbf{3}}, \mathbf{2}; -1/6\}, \{(\mathbf{8}, \mathbf{2}; 1/2), (\mathbf{3}, \mathbf{3}; -1/3), (\bar{\mathbf{3}}, \mathbf{2}; -1/6\}\}$
5	$-1 \cdot \{\{(\mathbf{6}, \mathbf{3}; 1/3), (\bar{\mathbf{6}}, \mathbf{1}; 1/3), (\mathbf{1}, \mathbf{3}; -1)\}, \{(\mathbf{6}, \mathbf{1}; 4/3), (\bar{\mathbf{6}}, \mathbf{3}; -1/3), (\mathbf{1}, \mathbf{3}; -1\}\}$ $2 \cdot \{\{(\mathbf{6}, \mathbf{3}; 1/3), (\bar{\mathbf{3}}, \mathbf{2}; -1/6), (\bar{\mathbf{3}}, \mathbf{2}; -1/6)\}, \{(\mathbf{3}, \mathbf{1}; -1/3), (\mathbf{3}, \mathbf{1}; -1/3), (\bar{\mathbf{6}}, \mathbf{1}; 2/3)\}, \{(\mathbf{3}, \mathbf{3}; -1/3), (\mathbf{3}, \mathbf{3}; -1/3), (\bar{\mathbf{6}}, \mathbf{1}; 2/3)\}\}$
7	$\{(\mathbf{8}, \mathbf{2}; 1/2), (\mathbf{8}, \mathbf{2}; 1/2), (\mathbf{1}, \mathbf{3}; -1)\}$ $-2 \cdot \{\{(\mathbf{8}, \mathbf{2}; 1/2), (\mathbf{3}, \mathbf{1}; -1/3), (\bar{\mathbf{3}}, \mathbf{2}; -1/6)\}, \{(\mathbf{8}, \mathbf{2}; 1/2), (\mathbf{3}, \mathbf{3}; -1/3), (\bar{\mathbf{3}}, \mathbf{2}; -1/6)\}\}$
11	$\{(\mathbf{8}, \mathbf{2}; 1/2), (\mathbf{3}, \mathbf{1}; 1/3), (\bar{\mathbf{3}}, \mathbf{2}; -1/6)\}$
16	$2 \cdot \{(\mathbf{3}, \mathbf{1}; -1/3), (\mathbf{3}, \mathbf{1}; -1/3), (\bar{\mathbf{6}}, \mathbf{1}; 2/3)\}$
17	$\{(\mathbf{8}, \mathbf{2}; 1/2), (\mathbf{3}, \mathbf{1}; -1/3), (\bar{\mathbf{3}}, \mathbf{2}; -1/6)\}$
22	$2 \cdot \{(\mathbf{6}, \mathbf{1}; 4/3), (\bar{\mathbf{3}}, \mathbf{2}; -7/6), (\bar{\mathbf{3}}, \mathbf{2}; -1/6)\}$
23	$\{(\mathbf{1}, \mathbf{2}; 1/2), (\mathbf{1}, \mathbf{2}; 1/2), (\mathbf{1}, \mathbf{3}; -1)\}$ $-2 \cdot \{\{(\mathbf{1}, \mathbf{2}; 1/2), (\mathbf{3}, \mathbf{1}; -1/3), (\bar{\mathbf{3}}, \mathbf{2}; -1/6)\}, \{(\mathbf{1}, \mathbf{2}; 1/2), (\mathbf{3}, \mathbf{3}; -1/3), (\bar{\mathbf{3}}, \mathbf{2}; -1/6)\}\}$
24	$\{(\mathbf{1}, \mathbf{2}; 1/2), (\mathbf{3}, \mathbf{1}; -1/3), (\bar{\mathbf{3}}, \mathbf{2}; -1/6)\}, \{(\mathbf{1}, \mathbf{2}; 1/2), (\mathbf{3}, \mathbf{3}; -1/3), (\bar{\mathbf{3}}, \mathbf{2}; -1/6)\}$ $-\frac{1}{2} \cdot \{(\mathbf{1}, \mathbf{2}; 1/2), (\mathbf{1}, \mathbf{2}; 1/2), (\mathbf{1}, \mathbf{3}; -1)\}$
26	$\{(\mathbf{1}, \mathbf{2}; 1/2), (\mathbf{3}, \mathbf{1}; -1/3), (\bar{\mathbf{3}}, \mathbf{2}; -1/6)\}$
27	$\{(\mathbf{1}, \mathbf{2}; 1/2), (\mathbf{3}, \mathbf{1}; -1/3), (\bar{\mathbf{3}}, \mathbf{2}; -1/6)\}$
28	$\frac{3}{2} \cdot \{(\mathbf{6}, \mathbf{1}; 4/3), (\bar{\mathbf{6}}, \mathbf{1}; 2/3), (\bar{\mathbf{1}}, \mathbf{1}; -2)\}$ $-3 \cdot \{(\mathbf{3}, \mathbf{1}; -1/3), (\bar{\mathbf{3}}, \mathbf{1}; -1/3), (\bar{\mathbf{6}}, \mathbf{1}; 2/3)\}$

[1] M. Fukugita and T. Yanagida, Phys. Lett. B **174**, 45 (1986).
[2] F. F. Deppisch, M. Hirsch, and H. Päs, J. Phys. G **39**, 124007 (2012).
[3] W. Rodejohann, Int. J. Mod. Phys. E **20**, 1833 (2011).
[4] A. Faessler, V. Rodin, and F. Simkovic, J. Phys. G **39**, 124006 (2012).
[5] F. Simkovic, Phys. Part. Nucl. Lett. **10**, 623 (2013).
[6] M. Agostini *et al.* (GERDA Collaboration), Phys. Rev. Lett. **111**, 122503 (2013).
[7] J. Albert *et al.* (EXO-200 Collaboration), Nature (London) **510**, 229 (2014).
[8] K. Asakura *et al.*, AIP Conf. Proc. **1666**, 170003 (2015).
[9] A. Gando *et al.* (KamLAND-Zen), Phys. Rev. Lett. **117**, 082503 (2016); **117**, 109903 (2016).
[10] M. Agostini *et al.* (GERDA Collaboration), *Presentation at Neutrino-2016, London, 2016* (unpublished).
[11] D. Auty (EXO-200 Collaboration), *48th Recontres de Moriond 2013, 2013* (unpublished).
[12] I. Abt *et al.* (GERDA Collaboration), arXiv:hep-ex/0404039.
[13] C. Aalseth *et al.* (Majorana Collaboration), Nucl. Phys. B, Proc. Suppl. **217**, 44 (2011).
[14] H. Päs, M. Hirsch, H. Klapdor-Kleingrothaus, and S. Kovalenko, Phys. Lett. B **453**, 194 (1999).
[15] H. Päs, M. Hirsch, H. Klapdor-Kleingrothaus, and S. Kovalenko, Phys. Lett. B **498**, 35 (2001).
[16] J. Helo, M. Hirsch, S. Kovalenko, and H. Päs, Phys. Rev. D **88**, 011901 (2013).
[17] J. Helo, M. Hirsch, H. Päs, and S. Kovalenko, Phys. Rev. D **88**, 073011 (2013).
[18] J. C. Helo, M. Hirsch, and S. Kovalenko, Phys. Rev. D **89**, 073005 (2014); **93**, 099902(E) (2016).
[19] J. C. Helo and M. Hirsch, Phys. Rev. D **92**, 073017 (2015).
[20] L. Gonzáles, J. C. Helo, M. Hirsch, and S. G. Kovalenko, J. High Energy Phys. 12 (**2016**) 130.
[21] N. Mahajan, Phys. Rev. Lett. **112**, 031804 (2014).
[22] M. González, M. Hirsch, and S. G. Kovalenko, Phys. Rev. D **93**, 013017 (2016).
[23] C. Arbeláez, M. González, M. Hirsch, and S. Kovalenko, Phys. Rev. D **94**, 096014 (2016).
[24] T. Peng, M. J. Ramsey-Musolf, and P. Winslow, Phys. Rev. D **93**, 093002 (2016).
[25] A. Faessler, S. Kovalenko, and F. Simkovic, Phys. Rev. D **58**, 055004 (1998).
[26] F. Bonnet, M. Hirsch, T. Ota, and W. Winter, J. High Energy Phys. 03 (2013) 055.
[27] G. Prezeau, M. Ramsey-Musolf, and P. Vogel, Phys. Rev. D **68**, 034016 (2003).
[28] M. Doi, T. Kotani, and E. Takasugi, Prog. Theor. Phys. Suppl. **83**, 1 (1985).
[29] M. Hirsch, K. Muto, T. Oda, and H. V. Klapdor-Kleingrothaus, Z. Phys. A **347**, 151 (1994).
[30] R. Mohapatra, Phys. Rev. D **34**, 3457 (1986).
[31] M. Hirsch, H. Klapdor-Kleingrothaus, and S. Kovalenko, Phys. Rev. D **53**, 1329 (1996).
[32] S. L. Adler, E. W. Colglazier, Jr., J. B. Healy, I. Karliner, J. Lieberman, Y. J. Ng, and H. S. Tsao, Phys. Rev. D **11**, 3309 (1975).
[33] T. Gutsche, M. A. Ivanov, J. G. Korner, S. Kovalenko, and V. E. Lyubovitskij, Phys. Rev. D **94**, 114030 (2016).